

GENETIC OPTIMISATION OF BEAMLINE DESIGN FOR DIAMOND

F. Bakkali Taheri[†], M. Apollonio, R. Bartolini, J. Li, B. Singh,
 Diamond Light Source, Oxfordshire, U.K.

Abstract

The problem of optimisation of beamline structures is studied, from the point of view of multi-objective genetic algorithms. While this approach has been successfully used in the exploration of potential particle accelerator lattices, it has never been applied to beamline design. In this paper, the Non-Dominated Sorting Genetic Algorithm II (NSGA II) is used to optimise a structure where photons are assumed to propagate through the optical elements according to a wave-front model. Examples illustrating this optimisation method are shown in the context of Diamond-II.

INTRODUCTION

The design of a beamline is a notoriously challenging task due to several aspects: the large number of degrees of freedom in the chain of optical components, the photon properties at the source, and the electron dynamics in the particle accelerator. Several tools are available to help the design of an operational beamline, and the choice usually depends on the underlying mathematical framework chosen to describe the radiation characteristics through the optical system. At Diamond Light Source the most common software used to simulate photon propagation are SHADOW [1], based on the geometrical framework of well-known raytracing methods, and Synchrotron Radiation Workshop (SRW) [2], which is based on the wave-front propagation theory and uses the full mathematical apparatus of Fourier optics. A major shortcoming of both these approaches, however, is that, while they allow to design a beamline, they do not guarantee that the final setup is actually the best configuration achievable. This is where the need for optimisation methods finds its justification. Recently there has been an increased interest in optimisation techniques in the context of beamline design. However, previous works on beamline optimisation address the problem by optimising a single quantity, and in the context of online system [3][4]. The work presented here is a contribution to an approach to beamline design that can accommodate an arbitrary number of optimisation requirements.

MULTI-OBJECTIVE OPTIMISATION

A multi-objective optimisation problem is a situation where a function $f : (p_1, p_2, \dots, p_N) \rightarrow (o_1, o_2, \dots, o_M)$ maps a set of parameters onto a set of objectives, the latter satisfying an extremum condition. The area of mathematics concerned with the exploration of such problems is very rich. A major result is that there exist iterative processes that exhibit an asymptotic convergence of the function f towards a stable hypersurface in the objective space, known

as Pareto front. Crucially, the method chosen to move from one iteration to the next, will define the algorithm of interest. In the case of this study, we have used the Non-Dominated Sorting Genetic Algorithm II (NSGA-II), a genetic algorithm which has become standard in many technical areas in the recent years. This means that the rules defining the progression from one iteration to the next, are based on the genetic processes governing the transition of species in the natural world, from one generation to the next. A detailed description of the algorithm can be found in [5].

THE I13 BEAMLINE

I13 is the first long beamline at Diamond dedicated to imaging and coherence [6]. Two independent branches operate in the energy range of 6 to 30 keV with spatial resolution on the micro-to-nano length-scale. The Imaging branch is dedicated to imaging and tomography with in line phase contrast and full-field microscopy on the micron to nano-length scale. The coherence branch reaches ultimate resolution exploiting imaging techniques in the reciprocal space. The experimental stations are located at 230 m from the source, to exploit the coherence properties of the source. The optical layout is optimized for beam stability and high optical quality to preserve the coherent radiation. A schematic top view of the beamline is shown in Fig. 1.

NUMERICAL RESULTS

In this section, the results of an optimisation of I13 under various conditions are presented. The objectives of interest are the horizontal and vertical beam size at the sample position. All simulations consisted in a set of 50 generations of 100 individuals each. The source utilized for these calculations is an ideal undulator with a period of 25 mm and a length of 2.7 m set to operate at the peak of the 9th harmonic (11.209 keV). The Twiss parameters at the source are reported in Table 1, and correspond to one of the lattices studied by the AP group in the framework of Diamond-II studies. SRW was used for beamline computations.

Table 1: Simulation Parameters of I13

| ϵ_x (pm.rad) | β_x (m) | α_x | β_y (m) | α_y | η_x (mm) | δE (%) |
|--------------------------|------------------|------------|------------------|------------|------------------|-------------------|
| 130 | 7.7 | -0.24 | 4.3 | -0.53 | -3.5 | 0.07 |

Two-Dimensional Optimisation

A first study shows the behaviour of the two objectives when the optimisation problem is posed in a 2-dimension parameter space, where the degrees of freedom are the last two drifts of the system (d_2 and d_3 in Fig. 1).

[†] faissal.bakkali-taheri@diamond.ac.uk

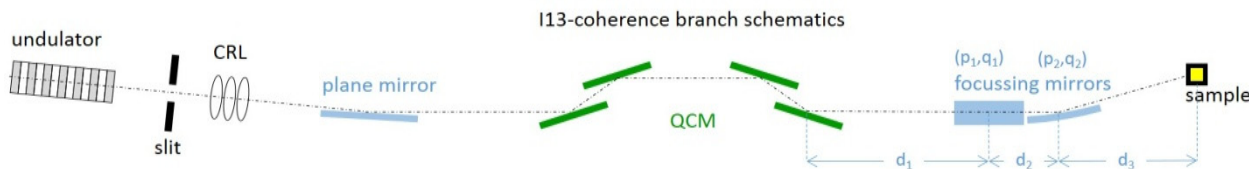


Figure 1: A schematic representation of I13-coherence branch (top view).

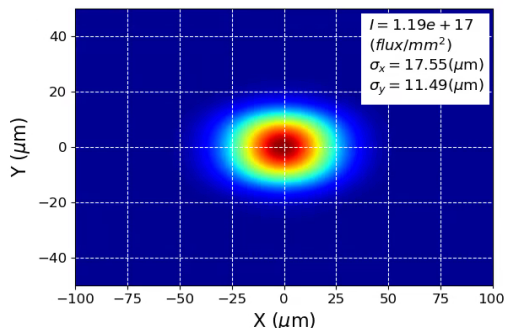


Figure 2: Beam size at sample for baseline beamline setup.

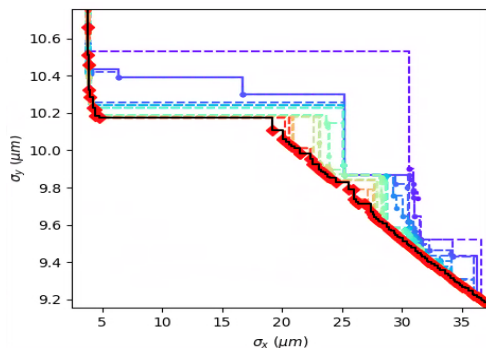


Figure 3: Pareto front of the 2D optimisation. Two distinct regions can be noticed in the top-left and bottom-right.

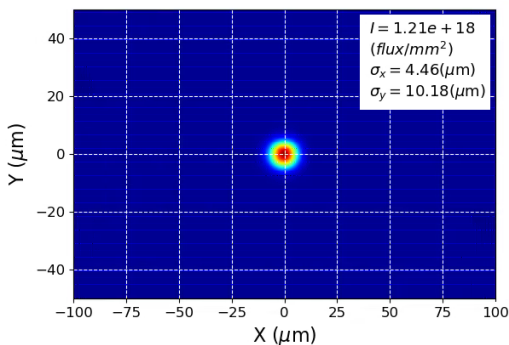


Figure 4: Beam size at sample after 2D optimisation.

Figure 2 shows the beam dimensions at sample position for the baseline configuration, before any optimisation takes place. From Fig. 3, it appears that the iteration fronts for this 2D-constrained dynamics converges towards an envelope, the Pareto front previously mentioned. In Fig. 4, a particular solution from the Pareto front has been extracted. It shows that in the process, the beam size can be reduced

from (17.5, 11.5) μm to (4.5, 10.2) μm , with a marginal improvement on the y-component.

In fact, the Pareto front shows that a particular feature of this 2D-parameter study, is that in most cases, only one component of the beam size can be reduced noticeably. The small number of parameters and the specific choice of d_2 and d_3 , acting on the horizontally focussing mirror of the KB system, are probably the reason for the limited effect on the vertical size of the beam and the formation of two distinct regions in the final front (see Fig. 3). The Table 2 shows that the optimisation is obtained for a set of parameters that is experimentally realistic.

Table 2: 2D-Optimisation of Beam Size

| | d_2 (m) | d_3 (m) | (σ_x, σ_y) ($\mu\text{m}, \mu\text{m}$) |
|-----------|-----------|-----------|---|
| baseline | 2.2 | 5.5 | (17.55, 11.49) |
| optimised | 1.32 | 5.92 | (4.46, 10.18) |

Seven-Dimensional Optimisation

The next step is therefore to see if the above results can be improved by extending the parameter space. To this purpose, five new degrees of freedom have been added to the two drifts used in the previous paragraph: the drift after the monochromator (d_1), and the focal distances of the two mirrors (p_i, q_i ; $i=1,2$). This sets up the multi-objective problem in a 7-dimensional parameters space. Figure 5 shows that the convergence envelope is considerably more regular.

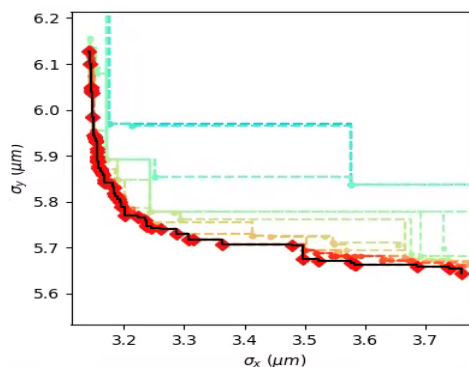


Figure 5: Pareto front of the 7D optimisation starting from the baseline configuration.

This time, unlike the previous case, no gap is present in the middle of the Pareto front, and it is now possible to improve the x and y dimensions of the beam size simultaneously. The outcome is shown in Fig. 6, where we see that the

initial beam dimensions of (17.5,11.5) μm has now significantly decreased to a stable minimum of (3.2,5.7) μm . The front density in that area shows that the genetic algorithm has essentially converged, and that improvements of higher order will be small, that is, there is no significant gain in leaving the genetic algorithm running longer. It is clear therefore that a higher number of degrees of freedom improves the optimisation. An important question that arises is how stable the solution we obtain is.

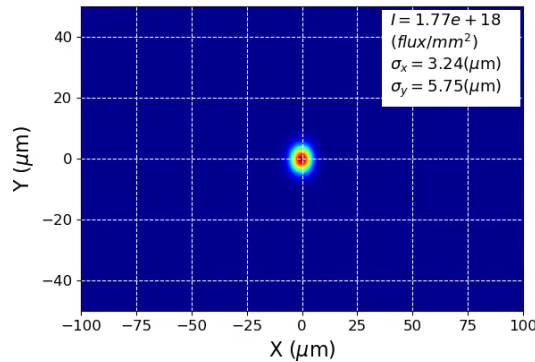


Figure 6: Beam size at sample after 7D optimisation starting from the baseline configuration.

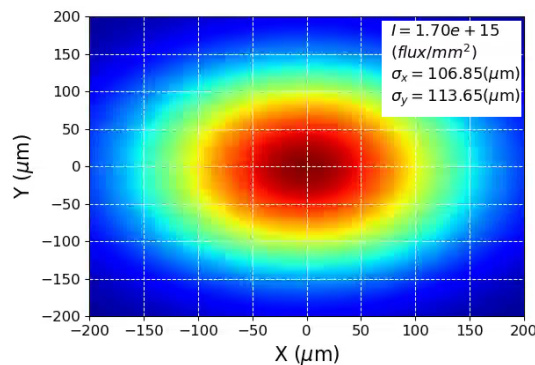


Figure 7: Beam size at sample before 7D optimisation starting from a random machine.

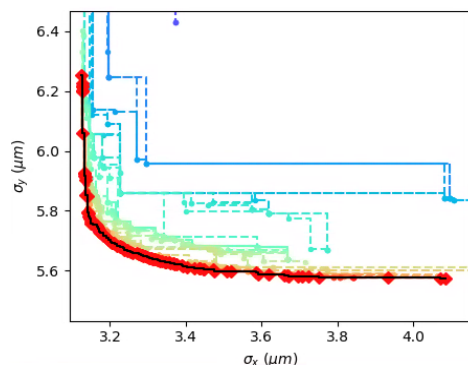


Figure 8: Pareto front of the 7D optimisation starting from a random machine configuration.

The previous 7D analysis shows that a continuous front optimisation of both objectives does exist, so, in a sense this is an empiric "existence" result. What we want to see

now is whether there would be the counterpart of an "empiric uniqueness", *i.e.* whether we would converge towards the same previously found solution, had the iteration process now started from a spoiled machine with a significantly different initial setting.

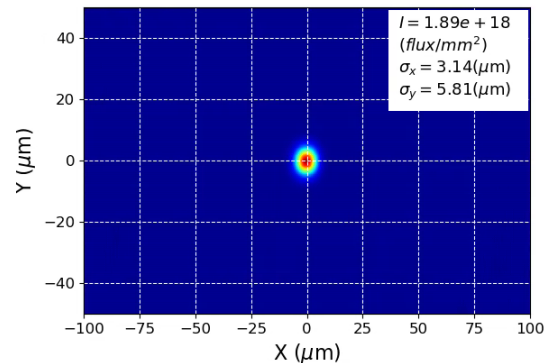


Figure 9: Beam size at sample after 7D optimisation starting from a random machine.

To explore this situation, the optimisation algorithm has been run this time starting from a random configuration, which initially yields a beam spot presented in Fig. 7 and where the dimensions are very large. The Pareto front of this version of the 7D-problem is shown in Fig. 8, and we see that the optimum pair observed in the bottom left of the front, displays sensibly similar values than in the study where we started from a realistic baseline configuration. The optimized beam spot for this case is presented in Fig. 9, and shows it is essentially the same solution that the one previously found. This suggests that the solution to the multi-objective optimisation of beamline depends on the parameter space that defines the geometry of the problem, and not the initial values of these parameters we start with. The Table 3 shows that, like in the 2D case, the optimization can be obtained for an experimentally realistic set of parameters.

Table 3: 7D-Optimisation of Beam Size

| | d ₁ , d ₂ , d ₃ (m, m, m) | p ₁ , p ₂ (m, m) | q ₁ , q ₂ (m, m) | (σ_x , σ_y) (μm , μm) |
|-----------------------------|---|---|---|--|
| baseline | 10, 2.2, 5.5 | 30.9, 9.1 | 33.1, 6.9 | 17.5, 11.4 |
| spoiled | 9.0, 3.8, 5.3 | 33.2, 5.2 | 33.8, 11 | 106, 113 |
| optimised | 10.7, 3.6, 5 | 33.9, 11.4 | 29.5, 5.8 | 3.24, 5.7 |
| optimised (from spoiled) | 12.9, 3.4, 5 | 34.1, 11.0 | 29.2, 5.8 | 3.14, 5.8 |

CONCLUSION

A robust algorithmic framework enabling multi-objective optimisation of a beamline was tested with on an arbitrary number of parameters, in a context where photon propagation is described using SRW. The optimized objectives depend on the number of degrees of freedom of the problem. It was also shown that, once the parameter space is defined, the Pareto convergence front is independent of the chosen initial configuration.

REFERENCES

- [1] M. Sanchez del Rio *et al.*, “SHADOW3: a new version of the synchrotron X-ray optics modelling package”, *J. Synchrotron Radiation*, vol. 18 (Pt 5), pp. 708–716, 2011.
- [2] O. Chubar and P. Elleaume, “Accurate and efficient computation of synchrotron radiation in the near field region”, in *Proc. EPAC’98*, Stockholm, Sweden, Jun. 1998, paper THP01G, pp. 1177–1179.
- [3] S. Appel *et al.*, “Automatized Optimisation of Beam Lines Using Evolutionary Algorithms”, in *Proc. 16th Int. Conf. on Accelerator and Large Experimental Control Systems (ICALEPCS’17)*, Barcelona, Spain, Oct. 2017, paper THPHA196, pp. 1906-1910. doi.org/10.18429/JACoW-ICALEPCS2017-THPHA196
- [4] S.Xi, L.S. Borgna, L. Zheng, Y. Du, and T.Hu, “AIBL-01.0: a program for automatic on-line beamline optimisation using the evolutionary algorithm”, *J. Synchrotron Rad.* (2017) <https://doi.org/10.1107/S1600577516018117>
- [5] K.Deb, A. Patrap, S. Agarwal, T. Meyariyan, “A fast and elitist multiobjective genetic algorithm: NSGA-IP”, *IEEE Trans. Evol. Comput.*, vol.6, No 2, pp. 182-197, 2002.
- [6] C.Rau, U. Wagner, A. Peach, I. K. Robinson, B. Singh, G. Wilkin, and C. Jones, “The Diamond Beamline I13L for Imaging and Coherence”, *AIP Conference Proceedings* 1234, 121 (2010). doi.org/10.1063/1.3463156

Content from this work may be used under the terms of the CC BY 3.0 licence (© 2019). Any distribution of this work must maintain attribution to the author(s), title of the work, publisher, and DOI